J. Phys.: Condens. Matter **22** (2010) 385501 (6pp) doi:10.1088/0953-8984/22/38/385501

Tuning independently the Fermi energy and spin splitting in Rashba systems: ternary surface alloys on Ag(111)

H Mirhosseini, A Ernst, S Ostanin and J Henk

Max-Planck-Institut für Mikrostrukturphysik, Weinberg 2, D-06120 Halle (Saale), Germany

E-mail: hossein@mpi-halle.de

Received 25 June 2010, in final form 2 August 2010
Published 3 September 2010
Online at stacks.iop.org/JPhysCM/22/385501

Abstract

By detailed first-principles calculations we show that the Fermi energy and the Rashba splitting in disordered ternary surface alloys $Bi_xPb_ySb_{1-x-y}$/Ag(111) can be independently tuned by choosing the concentrations x and y of Bi and Pb, respectively. The findings are explained by three fundamental mechanisms, namely the relaxation of the adatoms, the strength of the atomic spin–orbit coupling, and band filling. By mapping the Rashba characteristics, i.e. the splitting k_R and the Rashba energy E_R, and the Fermi energy of the surface states in the complete range of concentrations, we find that these quantities depend monotonically on x and y, with a very few exceptions. Our results suggest that we should investigate experimentally effects which rely on the Rashba spin–orbit coupling depending on spin–orbit splitting and band filling.

1. Introduction

In the emerging field of spin electronics, proposed device applications often utilize the Rashba effect [1] in a two-dimensional electron gas (2DEG). A prominent example is the spin field-effect transistor [2] in which the spin–orbit (SO) interaction in the 2DEG is controlled via a gate voltage [3, 4]. Other examples are a high critical superconducting temperature which shows up in materials with a sizable spin–orbit interaction [5] and the spin Hall effect [6–9].

The Rashba effect relies on breaking the inversion symmetry of the system and, consequently, shows up in semiconductor heterostructures and at surfaces. The breaking of the inversion symmetry results—via the spin–orbit coupling—in a splitting in the dispersion relation of electronic states which are confined to the interface [1]. In a simple model for a 2DEG, a potential in the z direction confines the electrons to the xy plane. The Hamiltonian of the spin–orbit coupling can thus be written as

$$\hat{H}_{so} = \gamma_R(\sigma_x\partial_y - \sigma_y\partial_x), \tag{1}$$

where the strength of the SO interaction is quantified by the Rashba parameter γ_R. Employing a plane-wave ansatz yields the dispersion relation

$$E_\pm(\vec{k}_\parallel) = E_0 + \frac{\hbar^2 k_\parallel^2}{2m^\star} \pm \gamma_R|\vec{k}_\parallel|, \tag{2}$$

where $m^\star$ is the effective electron mass. The split electronic states are labeled by $+$ and $-$; their spins lie within the xy plane, are aligned in opposite directions, and are perpendicular to the wavevector $\vec{k}_\parallel$.

In a real system, the Rashba parameter γ_R is comprised effectively of two contributions [10]. The 'atomic' contribution is due to the strong potential of the ions (atomic spin–orbit coupling). The 'confinement' contribution is due to the structural inversion asymmetry which can be viewed as the gradient of the confinement potential in the z direction. The larger this gradient and the atomic spin–orbit parameter, the larger γ_R and the splitting

$$k_R = \frac{|m^\star|\,\gamma_R}{\hbar^2}, \tag{3}$$

which is defined as the shift of the band extremum off the Brillouin zone center ($\vec{k}_\parallel = 0$). Another quantification of the splitting is the Rashba energy

$$E_R = -\frac{\hbar^2 k_R^2}{2m^\star} = -\frac{m^\star\gamma_R^2}{2\hbar^2}, \tag{4}$$

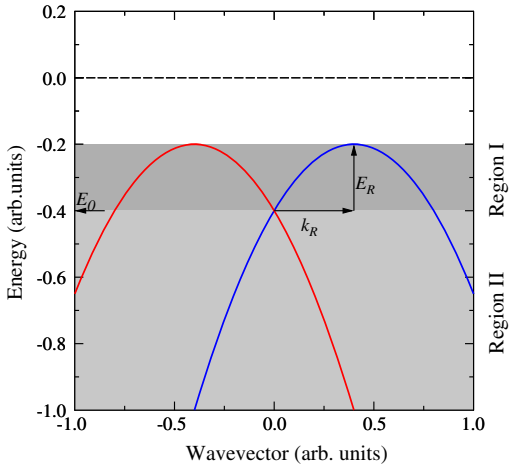

Figure 1. Schematic dispersion of Rashba-split surface states in a surface alloy, with negative effective mass $m^\star$. E_0, k_R, and E_R denote the crossing point of the bands at $k_\parallel = 0$, the splitting, and the Rashba energy, respectively. The spin orientation is indicated by the bands' colors (blue, red). The gray areas highlight the regions I (dark gray) and II (light gray).

that is the energy of the band extremum with respect to the energy E_0 for which the bands cross at $\vec{k}_\parallel = 0$ (figure 1).

The above dispersion relation suggests that we should distinguish two energy ranges. Region I is defined as the energy range between E_0 and the band extrema ($E \in [E_0 - E_\mathrm{R}, E_0]$ for positive $m^\star$ or $E \in [E_0, E_0 + E_\mathrm{R}]$ for negative $m^\star$) [11]. Region II comprises the other range of band energies ($E > E_0$ for positive $m^\star$ or $E < E_0$ for negative $m^\star$; figure 1). The density of states in region I is singular at the band extrema and decreases towards E_0 while in region II it is constant.

In view of designing device applications and investigating fundamental effects, it is desirable to tune both the strength γ_R of the Rashba spin–orbit coupling and the Fermi energy E_F of the 2DEG. In a semiconductor heterostructure, this can be achieved by an external gate voltage and by doping of the semiconductor host materials. At a surface, these quantities can be affected by adsorption of adatoms [12, 13], by surface alloying [11], and by changing the thickness of buffer layers (e.g. in Bi/(Ag)$_n$/Si(111) [14]). Recently, a ferroelectric control has been proposed [15].

Surface states in surface alloys show an unmatched Rashba splitting [16], as has been investigated in detail by scanning tunneling microscopy as well as by spin- and angle-resolved photoelectron spectroscopy. They are convenient systems for testing fundamental Rashba-based effects. The ordered surface alloys Bi/Ag(111), Pb/Ag(111), and Sb/Ag(111) have been investigated by first-principles calculations and in experiments [16–18]. These three systems differ with respect to their Rashba characteristics k_R and E_R, and by E_0. The challenge we are dealing with is how to tune these properties *independently*.

The basic idea is as follows. Bi/Ag(111) has a large splitting and occupied sp$_z$ surface states, while Pb/Ag(111) has a large splitting and unoccupied sp$_z$ surface states. In a disordered binary alloy Bi$_x$Pb$_{1-x}$/Ag(111) the Fermi energy can be tuned by the concentration x, while keeping a large spin splitting. In contrast, Sb/Ag(111) has occupied surface states with almost the same binding energy as those in Bi/Ag(111) but a minor splitting. This allows us to tune mainly the spin splitting but keeping the Fermi energy in Bi$_x$Sb$_{1-x}$/Ag(111). Thus, by an appropriate choice of concentrations x and y in a ternary alloy Bi$_x$Pb$_y$Sb$_{1-x-y}$/Ag(111) we expect to tune the Fermi energy and the splitting *independently*. In particular, one could access the region I between E_0 and the band maxima which is important for high-temperature superconductivity [5].

We report on a first-principles investigation of disordered surface alloys Bi$_x$Pb$_y$Sb$_{1-x-y}$/Ag(111), performed along the successful line of our previous works on both ordered and disordered alloys [11, 16, 18]. Since all ordered and disordered binary alloys show a $\sqrt{3} \times \sqrt{3}$R30° surface reconstruction, we assume this geometry also for the ternary alloys. The resulting substitutional disorder is described within the coherent potential approximation.

The paper is organized as follows. Our computational approach is sketched in section 2. The results are discussed in section 3, for binary alloys in section 3.4 and for ternary alloys in section 3.5. We give conclusions in section 4.

2. Computational aspects

We rely on our successful multi-code approach, based on the local density approximation to density functional theory. Because this is described in detail elsewhere [15], we deliberately only sketch it in this paper.

The surface relaxations of ordered surface alloys were determined using the Vienna *ab initio* Simulation Package (VASP) [19], well known for providing precise total energies and forces. The relaxed structural parameters serve as input for first-principles multiple-scattering calculations. Our Korringa–Kohn–Rostoker (KKR) method already proved successful for relativistic electronic-structure computations of Rashba systems [14, 20].

The central quantity in multiple-scattering theory is the Green function [21]

$$G(\vec{r}_n, \vec{r}'_m; E, \vec{k}) = \sum_{\Lambda\Lambda'} Z^n_\Lambda(\vec{r}_n; E)\tau^{nm}_{\Lambda\Lambda'}(E, \vec{k})Z^m_{\Lambda'}(\vec{r}'_m; E)^\star - \delta^{nm}\sum_\Lambda Z^n_\Lambda(\vec{r}_<; E)J^n_\Lambda(\vec{r}_>; E)^\star, \quad (5)$$

where Z and J are regular and irregular scattering solutions of sites n and m at energy E and wavevector $\vec{k}$, respectively. $\vec{r}_n$ is taken with respect to the position $\vec{R}_n$ of site n ($\vec{r}_n = \vec{r} - \vec{R}_n$). $r_<$ ($r_>$) is the lesser (larger) of r_n and r'_n. $\Lambda = (\kappa, \mu)$ comprises the relativistic spin-angular-momentum quantum numbers [21]. The scattering-path operator τ is obtained in standard KKR form from the so-called KKR equation [21] or in layer-KKR from the Dyson equation for the Green function [22].

The local electronic structure is analyzed in terms of the spectral density

$$N^n(E; \vec{k}) = -\frac{1}{\pi}\Im\mathrm{Tr}\, G(\vec{r}_n, \vec{r}_n; E, \vec{k}). \quad (6)$$

By taking appropriate decompositions of the trace, the spectral density provides information on the spin polarization and orbital composition of the electronic states.

Substitutional ternary alloys $Bi_xPb_ySb_{1-x-y}$/Ag(111) are described within the coherent potential approximation (KKR-CPA), in which short-range order is neglected. From the agreement of the theoretical data with their experimental counterparts for the binary alloys Bi_xPb_{1-x}/Ag(111) [11], we conclude that short-range order is of minor importance in these systems. Hence, we applied the KKR-CPA also for the ternary alloys.

The effect of the disorder can be understood as a self-energy [23]. As a consequence, the spectral density of the disordered alloys becomes blurred (or smeared out) as compared to that of the ordered alloys.

3. Results and discussion

3.1. Geometry

Relaxations have been determined by VASP for the ordered alloys, with $\sqrt{3} \times \sqrt{3}$R30° reconstruction and face-centered-cubic (fcc) stacking (VASP cannot treat substitutional disorder within the CPA). It turns out that the relaxations of Sb, Bi, and Pb are in accord with their atomic radii. To be more precise, the outward relaxations are 9.6, 15, and 18% of the Ag(111) bulk interlayer spacing (2.33 Å), respectively, with respect to the positions of the Ag atoms in the topmost layer. Being negligibly small, in-plane displacements of Ag atoms are not considered.

Since all ordered and disordered binary alloys show a $\sqrt{3}\times\sqrt{3}$R30° surface reconstruction, we assume this geometry also for the ternary alloys. The relaxations of the disordered surface alloys were linearly interpolated, depending on the concentrations of the constituting elements Bi, Pb, and Sb. This assumption is within the spirit of the CPA; being a mean-field theory, a disordered system is described by an effective medium. Likewise the relaxation should be taken as a concentration-weighted average. We are aware, however, that in real samples, the relaxations of the constituting individual atoms could differ, as might be checked by scanning tunneling microscopy.

3.2. Mechanisms which influence the Rashba-split surface states

Before presenting details of our calculations, a brief discussion of the general trends and mechanisms is in order. For tuning the Fermi energy and spin splitting independently, the underlying mechanisms should be independent as well.

A first mechanism is relaxation. The outward relaxations of Sb, Pb, and Bi are in accord with their atomic radii; the larger the atomic radius, the larger the outward relaxation. The relaxation is accompanied by a charge transfer from the atomic sphere to the surrounding: the larger the relaxation, the larger the charge transfer [24]. This mechanism determines mainly the energy position of the degenerate point E_0—compare with (2) and figure 1—and, consequently, the Fermi energy or band filling of the surface states (2DEG).

A second mechanism is the atomic spin–orbit parameter. Bi and Pb are heavy elements with large SO parameter (1.25 eV for Bi and 0.91 eV for Pb [25]), in contrast to the lighter element Sb (0.4 eV [25]). The Rashba splitting depends both on the atomic SO-coupling strength and the potential gradient [10]. Since the latter should not differ considerably among the considered systems, the spin splitting is mainly determined by the atomic SO coupling. We expect that with increasing Sb content, the spin splitting should decrease.

A third mechanism is electron doping or band filling. Pb has one valence electron less than the isoelectronic elements Bi and Sb ($Z_{Pb} = 82$, $Z_{Bi} = 83$, $Z_{Sb} = 51$). Within a rigid-band model, the surface states in Pb/Ag(111) are shifted to higher energies, as compared to those in Bi/Ag(111) and Sb/Ag(111). This picture is confirmed by experiments and first-principles calculations [11, 26].

Note that the splitting k_R and the Rashba energy E_R are not fully independent. A relaxation, for example, can induce modification of both k_R and E_R.

3.3. Ordered surface alloys

The ordered surface alloys Bi/Ag(111), Pb/Ag(111), and Sb/Ag(111) have been studied previously in detail [16–18]. They show two sets of surface states; a first set is unoccupied and consists mainly of p_xp_y orbitals (for Bi/Cu(111), see [27]). In this paper, we focus on the other set which is either completely or partially occupied and consists of sp_z orbitals. The effective mass $m^\star$ of both sets is negative, implying a negative dispersion (compare with figure 1).

3.3.1. Sb/Ag(111). We address briefly the above-mentioned relaxation mechanism by considering two cases for Sb/Ag(111): (i) an Sb relaxation as calculated by VASP (9.6%) and (ii) an artificial relaxation of 25%. The charge transfer from the Sb muffin-tin spheres to the surrounding is increased for the larger relaxation (2.05% as compared to 0.94%, with respect to the nominal valence charge; compare with [24]). Consequently, the surface states are shifted towards higher energies by 0.16 eV, as obtained from the degeneracy point E_0. Further, the spin splitting k_R becomes increased as well (0.03 $Å^{-1}$ as compared to 0.02 $Å^{-1}$). This corroborates that the relaxation mainly affects the crossing point E_0 (or Fermi energy) rather than the spin splitting.

3.4. Disordered binary alloys

3.4.1. Bi_xPb_{1-x}/Ag(111). In the disordered binary alloy Bi_xPb_{1-x}/Ag(111), which has been studied previously [11], the ratio of the Rashba energy E_R and the Fermi energy E_F can be chosen within a wide range, depending on the Bi concentration x. For both Bi and Pb, 0.99% of the atomic charge atom is removed from the muffin-tin sphere, which is in agreement with the close outward relaxation of Bi and Pb (15% and 18%). As noted before, Pb has one valence electron less than Bi, which explains the sizable shift of the surface states to higher energies (band-filling mechanism; compare with the panels on the right-hand side of figure 2). Although

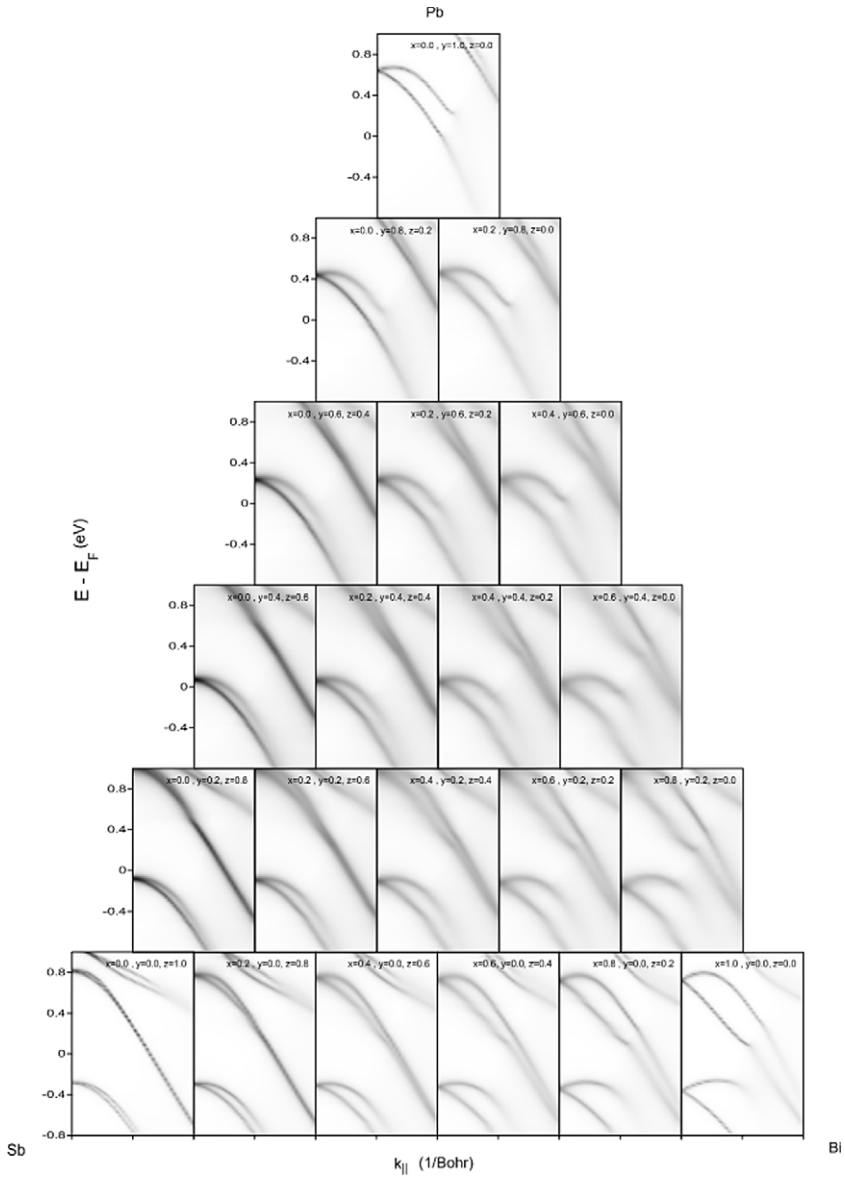

Figure 2. Surface states of disordered ternary alloys $Bi_xPb_ySb_{1-x-y}$/Ag(111) along $\bar{\Gamma}$–$\bar{K}$ of the two-dimensional Brillouin zone. The spectral density at a heavy-element site $Bi_xPb_ySb_{1-x-y}$ is depicted as linear gray scale, with dark gray corresponding to high spectral weight; compare with (6).

the relaxation is of the same order, the splitting is smaller for Pb (topmost panel in figure 2). This can be attributed to the smaller atomic spin–orbit parameter of Pb (0.91 eV for Pb and 1.25 eV for Bi [25]).

3.4.2. Bi_xSb_{1-x}/Ag(111). Recently, the surface states of the disordered binary alloys Bi_xSb_{1-x}/Ag(111) were mapped out by angle-resolved photoelectron spectroscopy. The momentum offset k_R evolves continuously with increasing Bi concentration x. The splitting decreases sizably for $x < 0.50$ [28].

In theory, the outward relaxation of Bi is larger than for the Sb (15% and 9.6%, respectively). Consequently the charge which is removed from the Sb sphere (0.94%) is slightly smaller than that of Bi (0.99%). Since Bi and Sb are isoelectronic, with valence-shell configuration $5p^3$ and $6p^3$, E_0 remains almost unaffected by x, as can be seen in the bottom row of figure 2. The spin splitting for Sb is much less than for Bi, in agreement with the atomic spin–orbit parameter (0.4 and 1.25 eV). In accord with experimental results, the Rashba splitting k_R evolves with Bi concentration x.

To elucidate further the effect of the relaxation, we calculated the splitting of $Bi_{0.6}Sb_{0.4}$/Ag(111) for two relaxations. The interpolated relaxation for $Bi_{0.6}Sb_{0.4}$/Ag(111) is 12.8% (shown at $(x, y, z) = (0.6, 0.4, 0.0)$ in figure 2), for the artificial relaxed system the outward relaxation is taken as 19% (not shown here). The charge transfer for the two systems is very close, and the difference in the splitting is negligibly small. Hence, the splitting is negligibly sensitive to the relaxation, as was already established for Sb/Ag(111).

3.4.3. Pb_ySb_{1-y}/Ag(111). To complete the picture of the binary alloys we turn to Pb_ySb_{1-y}/Ag(111), for which

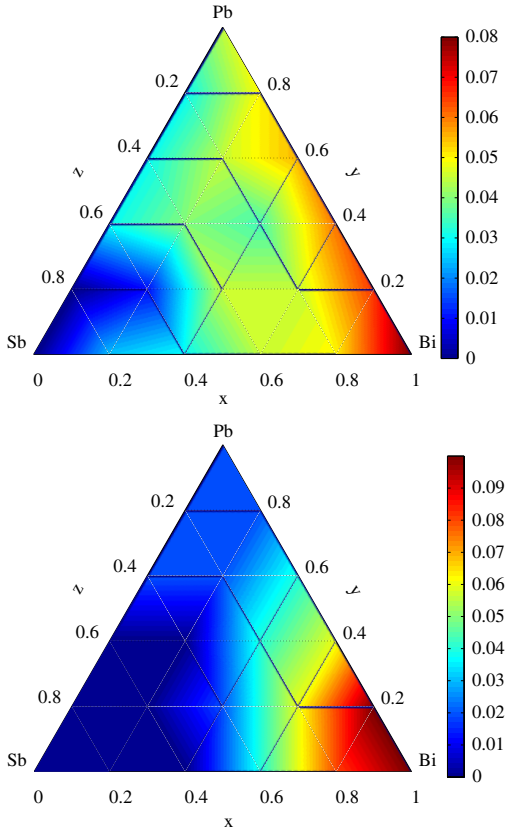

Figure 3. Spin splitting in disordered ternary alloys $Bi_xPb_ySb_{1-x-y}$/Ag(111). Top: the surface-state displacement k_R (in reciprocal space) is depicted on a color scale as a function of Bi concentration x, Pb concentration y, and Sb concentration $z = 1 - x - y$. The color bar on the right is in units of $Å^{-1}$. Bottom: the same as in the top but for the Rashba energy E_R. The color bar is in electronvolt.

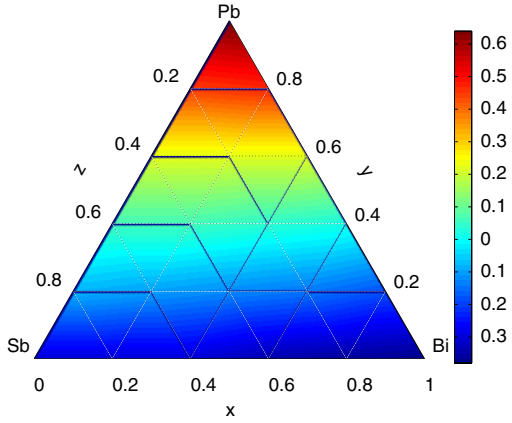

Figure 4. Surface-state energy in disordered ternary alloys $Bi_xPb_ySb_{1-x-y}$/Ag(111). The degeneracy energy E_0 of the surface state, with respect to the Fermi level E_F, is depicted on a color scale as a function of Bi concentration x, Pb concentration y, and Sb concentration $z = 1 - x - y$. The color bar on the right is in electronvolt. At negative energies, the surface states are fully occupied (blue area).

experimental results are not available. The trends which have been discussed before are also found in these alloys (compare with the panels on the left-hand side of figure 2). As the Pb concentration increases, E_0 shifts down from $E_F + 0.6$ eV to $E_F - 0.4$ eV, implying that the surface states become completely filled at about $y = 0.3$. As for Bi_xSb_{1-x}/Ag(111), the spin splitting increases with y.

3.5. Disordered ternary alloys $Bi_xPb_ySb_{1-x-y}$/Ag(111)

Having established the ingredients which are necessary for independently tuning the Fermi energy and the spin splitting in the surface alloys—by investigating the disordered binary surface alloys—we now mix them to disordered ternary alloys $Bi_xPb_ySb_{1-x-y}$/Ag(111). By choosing appropriate concentrations x and y, the degeneracy point E_0 and the Rashba splitting are tuned. Note that the splitting k_R and the Rashba energy E_R are not fully independent; both can be expressed (in a free-electron model) in terms of the effective electron mass and the Rashba parameter (compare with (3) and (4)).

In figure 2 the surface-state dispersions of ternary alloys $Bi_xPb_ySb_{1-x-y}$/Ag(111) are shown. The concentrations x and y have been varied in steps of 0.2. A common feature of the spectral density of the binary and ternary alloys is a finite lifetime of the spectral density, which is a consequence of the substitutional disorder.

The Rashba characteristics of the ternary alloys follow the general trends of the binary alloys which have been discussed before. In the ternary alloys with larger outward relaxation (i.e. the Bi- and Pb-rich compounds), the degenerate point E_0 shifts toward higher energies (main mechanism: relaxation). The larger the concentration of heavy elements Bi and Pb as compared to the Sb concentration, the larger the splitting k_R (main mechanism: atomic spin–orbit parameter). The degenerate point E_0 shifts upward with increasing Pb concentration (main mechanism: band filling).

The shift k_R of the surface states in reciprocal space versus concentrations x and y is shown in figure 3 (top). As expected, the smallest splitting (dark blue) shows up for Sb/Ag(111) ($z = 1 - x - y = 1$), while the largest (dark red) corresponds to Bi/Ag(111) ($x = 1$). For Pb/Ag(111), k_R is of intermediate order (green/yellow). Surprisingly, the splitting is not monotonic, as one might have expected in a rigid-band picture. For example, k_R shows a local minimum at $(x, y, z) \approx (0.4, 0.4, 0.2)$.

As k_R, the Rashba energy E_R depends monotonously in a large range of concentrations (bottom in figure 3). Sizable Rashba energies are found mainly for Bi-rich alloys, say for $x > 0.5$. This implies that for accessing region I, Bi-rich surface alloys are inevitable. For smaller x (blue areas in the bottom panel of figure 3), the energy range of region I could be too small to be employed in experiments.

The energy E_0 of the degeneracy point depends almost linearly on the heavy elements' concentrations x and y (figure 4). For equal Bi and Sb concentrations ($x = z$) it is nearly constant; upon adding Pb, E_0 shifts up. For systems with about 40% of Pb concentration, E_0 is very close to the Fermi level E_F, so that the latter lies in region I [24].

In summary, the above results support the fact that both Fermi energy and spin splitting in the surface states can be tuned independently, as is readily apparent from the different shapes in figures 3 and 4. A very interesting region in the ternary plots is around $(x, y, z) \approx (0.6, 0.3, 0.1)$, where the degenerate point E_0 and the Fermi energy E_F coincide. Keeping the Sb concentration constant and changing the Pb concentration of about 10% is accompanied by transition between region I and region II, while k_R and E_R are almost constant. It is also possible to tune E_R and k_R while keeping the position of the degenerate point constant. The changes of k_R and E_R are not independent but k_R depends more sensitively on the concentrations than E_R.

4. Conclusions

Disordered ternary surface alloys $Bi_xPb_ySb_{1-x-y}$/Ag(111) allow us to fabricate a 2DEG with specific Rashba spin–orbit splitting and Fermi energy which can be investigated by surface-scientific methods (scanning tunneling probes and especially photoelectron spectroscopy). In particular, the important transition from energy region I (that is where the Fermi energy E_F lies above the degeneracy point E_0) to region II (E_F below E_0) can be studied for different strengths of the Rashba spin–orbit coupling. Thus, the present study may stimulate further experiments on Rashba systems and their unique properties.

Acknowledgments

We gratefully acknowledge very fruitful discussions with Christian Ast, Hugo J Dil, Isabella Gierz, and Fabian Meier.

References

[1] Bychkov Yu A and Rashba É I 1984 Properties of a 2D electron gas with lifted degeneracy *Sov. Phys. JETP Lett.* **39** 78 (translated from Ref. Bychkov84c)
[2] Datta S and Das B 1990 Electronic analogue of the electronic modulator *Appl. Phys. Lett.* **56** 665
[3] Nitta J, Akazaki T, Takayanagi H and Enoki T 1997 Gate control of spin–orbit interaction in an inverted $In_{0.53}Ga_{0.47}As/In_{0.52}Al_{0.48}As$ heterostructure *Phys. Rev. Lett.* **78** 1335
[4] Koga T, Nitta J, Takayanagi H and Datta S 2002 Spin-filter device based on the Rashba effect using a nonmagnetic resonant tunneling diode *Phys. Rev. Lett.* **88** 126601
[5] Cappelluti E, Grimaldi C and Marsiglio F 2007 Topological change of the Fermi surface in low-density Rashba gases: application to superconductivity *Phys. Rev. Lett.* **98** 167002
[6] Hirsch J E 1999 Spin Hall effect *Phys. Rev. Lett.* **83** 1834
[7] Kato Y, Myers R C, Gossard A C and Awschalom D D 2004 Coherent spin manipulation without magnetic fields in strained semiconductors *Nature* **427** 50
[8] Saraga D S and Loss D 2005 Fermi liquid parameters in two dimensions with spin–orbit interaction *Phys. Rev.* B **72** 195319
[9] Valenzuela S O and Tinkham M 2006 Direct electronic measurement of the spin Hall effect *Nature* **442** 176
[10] Petersen L and Hedegård P 2000 A simple tight-binding model of spin–orbit splitting of sp-derived surface states *Surf. Sci.* **459** 49
[11] Ast C R, Pacilé D, Moreschini L, Falub M C, Papagno M, Kern K, Grioni M, Henk J, Ernst A, Ostanin S and Bruno P 2008 Spin–orbit split two-dimensional electron gas with tunable Rashba and Fermi energy *Phys. Rev.* B **77** 081407(R)
[12] Forster F, Hüfner S and Reinert F 2004 Rare gases on noble-metal surfaces: an angle-resolved photoemission study with high energy resolution *J. Phys. Chem.* B **108** 14692
[13] Moreschini L, Bendounan A, Ast C R, Reinert F, Falub M and Grioni M 2008 Effect of rare-gas adsorption on the spin–orbit split bands of a surface alloy: Xe on Ag(111)–$(\sqrt{3} \times \sqrt{3})$R30°–Bi *Phys. Rev.* B **77** 115407
[14] Frantzeskakis E, Pons S, Mirhosseini H, Henk J, Ast C R and Grioni M 2008 Tunable spin gaps in a quantum-confined geometry *Phys. Rev. Lett.* **101** 196805
[15] Mirhosseini H, Maznichenko I V, Abdelouahed S, Ostanin S, Ernst A, Mertig I and Henk J 2010 Toward a ferroelectric control of rashba spin–orbit coupling: Bi on *batio*3(001) from first principles *Phys. Rev.* B **81** 073406
[16] Ast C R, Henk J, Ernst A, Moreschini L, Falub M C, Pacilé D, Bruno P, Kern K and Grioni M 2007 Giant spin splitting through surface alloying *Phys. Rev. Lett.* **98** 186807
[17] Bihlmayer G, Blügel S and Chulkov E V 2007 Enhanced Rashba spin–orbit splitting in Bi/Ag(111) and Pb/Ag(111) surface alloys *Phys. Rev.* B **75** 195414
[18] Moreschini L, Bendounan A, Gierz I, Ast C A, Mirhosseini H, Höchst H, Kern K, Henk J, Ernst A, Ostanin S, Reinert F and Grioni M 2009 Assessing the atomic contribution to the Rashba spin–orbit splitting in surface alloys: Sb/Ag(111) *Phys. Rev.* B **79** 075424
[19] Kresse G and Furthmüller J 1996 Efficient iterative schemes for *ab initio* total-energy calculations using a plane-wave basis set *Phys. Rev.* B **54** 11169
[20] Henk J, Ernst A and Bruno P 2004 Spin polarization of the L-gap surface states on Au(111): a first-principles investigation *Surf. Sci.* **566–568** 482
[21] Zabloudil J, Hammerling R, Szunyogh L and Weinberger P (ed) 2005 *Electron Scattering in Solid Matter* (Berlin: Springer)
[22] Henk J 2001 Theory of low-energy diffraction and photoelectron spectroscopy from ultra-thin films *Handbook of Thin Film Materials* vol 2, ed H S Nalwa (San Diego, CA: Academic) chapter 10, p 479
[23] Weinberger P 1990 *Electron Scattering Theory of Ordered and Disordered Matter* (Oxford: Clarendon)
[24] Moreschini L, Bendounan A, Bentmann H, Assig M, Kern K, Reinert F, Henk J, Ast C R and Grioni M 2009 Influence of the substrate on the spin–orbit splitting in surface alloys on (111) noble-metal surfaces *Phys. Rev.* B **80** 035438
[25] Wittel K and Manne R 1974 Accurate calculation of ground-state energies in an analytic Lanczos expansion *Theor. chim. Acta.* **33** 347
[26] Bentmann H, Forster F, Bihlmayer G, Chulkov E V, Moreschini L, Grioni M and Reinert F 2009 Origin and manipulation of the Rashba splitting in surface alloys *Europhys. Lett.* **87** 37003
[27] Mirhosseini H, Henk J, Ernst A, Ostanin S, Chiang C-T, Yu P, Winkelmann A and Kirschner J 2009 Unconventional spin topology in surface alloys with Rashba-type spin splitting *Phys. Rev.* B **79** 245428
[28] Ast C R, Dil H J, Gierz I and Meier F 2010 private communication